Not All hERG Pore Domain Mutations Have a Severe Phenotype: G584S Has an Inactivation Gating Defect with Mild Phenotype Compared to G572S, Which Has a Dominant Negative Trafficking Defect and a Severe Phenotype

JING TING ZHAO, PH.D.,* ADAM P. HILL, PH.D.,*,† ANTHONY VARGHESE, PH.D.,‡
ANTONY A. COOPER, PH.D.,§ HEIKKI SWAN, M.D., PH.D.,¶
PÄIVI J. LAITINEN-FORSBLOM, PH.D.,** MARK I. REES, PH.D.,††,‡‡
JONATHAN R. SKINNER, M.D.,§§ TERENCE J. CAMPBELL, D.PHIL., M.D.,*,†
and JAMIE I. VANDENBERG, M.B.B.S., PH.D.*,†

From the *Victor Chang Cardiac Research Institute, Sydney, Australia; †St. Vincent's Clinical School, University of New South Wales, Sydney, Australia; ‡University of Wisconsin, River Falls, Wisconsin, USA; §Garvan Institute of Medical Research, Sydney, Australia; ¶Department of Cardiology, Helsinki University Central Hospital, Helsinki, Finland; **Department of Medicine, University of Helsinki, Helsinki, Finland; ††Institute of Life Science, School of Medicine, Swansea University, Swansea, UK; ‡‡Institute of Medical Genetics, School of Medicine, Cardiff University, Cardiff, UK; and §§Cardiac Inherited Disease Group, Starship Hospital, Auckland, New Zealand

Distinct Phenotypes in hERG Pore Domain Mutations. ***Introduction:*** **Mutations in the pore domain of the human *ether-a-go-go*-related gene (hERG) potassium channel are associated with higher risk of sudden death. However, in many kindreds clinical presentation is variable, making it hard to predict risk. We hypothesized that *in vitro* phenotyping of the intrinsic severity of individual mutations can assist with risk stratification.**

Methods and Results: **We analyzed 2 hERG pore domain mutations, G572S and G584S. Similar to 90% of hERG missense mutations, G572S-hERG subunits did not traffic to the plasma membrane but could coassemble with WT subunits and resulted in a dominant negative suppression of hERG current density. The G584S-hERG subunits traffic normally but have abnormal inactivation gating. Computer models of human ventricular myocyte action potentials (AP), incorporating Markov models of the hERG mutants, indicate that G572S-hERG channels would cause more severe AP prolongation than that seen with G584S-hERG channels.**

Conclusions: **hERG-G572S and -G584S are 2 pore domain mutations that involve the same change in sidechain but have very different *in vitro* phenotypes; G572S causes a dominant negative trafficking defect, whereas G584S is the first hERG missense mutation where the cause of disease can be exclusively attributed to enhanced inactivation. The G572S mutation is intrinsically more severe than the G584S mutation, consistent with the overall clinical presentation in the 2 small kindreds studied here. Further investigation, involving a larger number of cohorts, to test the hypothesis that *in vitro* phenotyping of the intrinsic severity of a given mutation will assist with risk stratification is therefore warranted.** *(J Cardiovasc Electrophysiol, Vol. 20, pp. 923-930, August 2009)*

long-QT syndrome, protein trafficking, kinetic modeling, arrhythmia, human ether-a-go-go-related gene

Introduction

Patients with congenital long-QT syndrome (LQTS) are a well-characterized subset of patients at risk of sudden death, associated with prolongation of the QT interval on the surface electrocardiogram and ventricular arrhythmias in the context of a structurally normal heart.[1] Over the last 10 years, studies on the long-QT registry population[2] have led to the identification of a number of markers associated with an increased risk of cardiac events in patients with LQTS. Clinical features including male gender in children[3,4] but female gender in adults[4,5] and a prior history of syncope[3] are associated with increased risk. Additionally, a corrected QT interval (QTc) duration greater than 500 ms[6] is associated with increased risk. However, in many instances affected kindreds are small and present with variable features making it hard to predict risk.

Approximately 95% of genotype-positive cases of LQTS are due to mutations in 3 genes, *KCNQ1, KCNH2,* and

Dr. Zhao and Dr. Hill contributed equally to this work.

This work was supported in part by grants from the St. Vincent's Clinic Foundation (to TJC), the National Heart Foundation of Australia (GIA G06S2585 to JIV, JRS, and MIR), and the National Health and Medical Research Council (NHMRC 459402, 573715 to JIV). APH is supported by a NHFA post-doctoral fellowship (Gxxxxxxx). JIV is supported by an NHMRC Senior Research Fellowship (NHMRC 459401). JRS and MIR are supported by Cure Kids of New Zealand and the Green Lane Trust.

Address for correspondence: Jamie I. Vandenberg, M.B.B.S., Ph.D., Victor Chang Cardiac Research Institute, 405 Liverpool Street, Darlighurst, NSW 2010, Australia. Fax: +61-2-92958770; E-mail: j.vandenberg@victorchang.edu.au

Manuscript received 17 December 2008; Revised manuscript received 2 February 2009; Accepted for publication 9 February 2009.

doi: 10.1111/j.1540-8167.2009.01468.x

SCN5A,[7] which encode for the pore-forming subunits of the slow component of the delayed rectifier K^+ channel (LQTS1; ~45%), the rapid component of the delayed rectifier K^+ channel (LQTS2; ~40%), and the cardiac sodium channel (LQTS3; ~10%), respectively. At a genetic level, mutations in *KCNQ1* and *KCNH2* are associated with more frequent events; however, a greater proportion of events in patients with mutations in *SCN5A* are lethal.[8] Even within a single locus, however, some genotypes are more lethal than others.[9] Mutation-specific genotype-phenotype relationships have been extensively characterized for KCNQ1 mutations, where mutations in the transmembrane domains[10] and mutations with a dominant negative phenotype[11] have a more malignant phenotype. In general, mutations in the pore-domain of hERG (encoded for by *KCNH2*) carry a greater risk of severe clinical outcomes compared to mutations in nonpore regions.[2]

In addition to using clinical markers (QT duration, age of onset, frequency of symptoms), individual mutations can be characterized *in vitro* using cellular electrophysiology assays.[12] *In vitro* cell-based assays have the potential to provide much more quantitative information on specific mutations. This has led to significant interest in utilizing biophysical characterization of mutants to help stratify risk.[13,14] Until recently, most studies on hERG channel mutations suggested that defective gating mutants were the most prominent cause of LQTS2.[12] One of the reasons for this is that the *in vitro* assay system of choice for characterizing ion channel function (due to ease of use and relatively high throughput analysis) has been heterologous expression in Xenopus laevis oocytes.[15] However, as Xenopus laevis oocytes are incubated at low temperatures (typically ~17°C), many mutant proteins that would be misfolded and consequently degraded in mammalian systems maintained at 37°C can instead reach the cell membrane in Xenopus laevis oocytes. More recently, it has been shown that >80% of LQTS associated hERG missense mutants, when expressed in mammalian cells, exhibit a trafficking defect.[16] The most important implication of these results is that it is essential when characterizing mutant channels to perform assays in mammalian cells.

Here, we show that the in vitro phenotype of 2 hERG pore domain mutations, G572S[17] and G584S,[18] both located in the short linker between the fifth transmembrane domain and the S5-P α-helix of the pore domain have very different phenotypes: a dominant negative trafficking defect for the G572S mutation compared to abnormal inactivation for the G584S mutation. The G572S mutant is therefore typical of the vast majority of missense mutations in hERG, but the G584S mutation represents the first missense mutation, characterized in mammalian systems, where enhanced inactivation is the cause of disease. These results also illustrate how 2 apparently similar genotypes can have very different molecular phenotypes and underscore the value of characterizing the biophysical properties of individual mutations.

Methods

Molecular Biology

DNA was extracted from blood samples using standard phenol-chloroform extraction. The coding sequences and splicing sites of LQTS genes *KCNQ1*, *KCNH2*, *SCN5A*, *KCNE1,* and *KCNE2* were screened for genomic variants as previously described.[17,18] The studies conform with the principles outlined in the Declaration of Helsinki and approval was obtained from the appropriate regional ethics committees.

hERG mutations and epitope-tagged constructs were generated by site-directed mutagenesis as previously described.[19] Both HA (YPYDVPDYA) and Flag (DYKDDDDK) epitopes were inserted in frame at the COOH-terminus of the hERG cDNA (a kind gift from Gail Robertson, University of Wisconsin). Constructs were confirmed by bidirectional sequencing.

Human embryonic kidney (HEK) 293 cells and Chinese Hamster Ovary (CHO) cells were transiently transfected with WT or mutant plasmids using either Effectene or Polyfect (both from Qiagen, VIC, Australia) as per manufacturer's protocol. Cells were cultured for 48 hours before electrophysiology or protein assays were performed.

Cell Biology

Western blotting

Proteins extracted from transfected HEK 293 cells were separated on 8% SDS-PAGE gels, transferred onto PVDF membranes and blocked overnight with 5% nonfat dry milk in TBS buffer. Membranes were immunoblotted with monoclonal mouse antibodies 1 hour at RT (anti-HA, Covance, Princeton, NJ, USA; 1:5,000 dilution or anti-Flag, Sigma, NSW, Australia; 1:1,000 dilution; 1 hour at RT). We used a horseradish peroxidase-conjugated secondary antibody for detection using the ECL system (GE Healthcare, Little Chalfont, UK) or fluorescently labeled IRDye 680 goat anti-mouse secondary antibody for detection using the Odyssey Infrared Imaging System (Li-COR Biosciences, Lincoln, NE, USA).

Immunoprecipitation

Whole-cell lysate from transfected HEK 293 cells was immunoprecipitated with anti-HA antibody and coprecipitated proteins detected by Western blot analysis with anti-Flag antibody.

Immunofluorescence microscopy

Transfected HEK 293 cells, grown on coverslips, were fixed with 4% paraformaldehyde in PBS, permeabilized with 0.2% Triton X-100 in PBS and blocked with 10% BSA buffer before incubation with anti-HA (rabbit) polyclonal and/or anti-Flag (mouse) monoclonal primary antibody (1:200) at 4°C overnight. Cells were washed with PBS than incubated with Cy3-conjugated donkey anti-mouse IgG secondary antibody and Cy5-conjugated donkey anti-rabbit IgG secondary antibody (Jackson Immunoresearch, West Grove, PA, USA) for 1 hour at room temperature.

Patch Clamp Electrophysiology

HERG currents were measured using the whole-cell patch-clamp technique, as described previously.[20] CHO cells were superfused with normal Tyrode's solution (mM: 130 NaCl, 4.8 KCl, 0.3 NaH_2PO_4, 0.3 KH_2PO_4, 1 $MgCl_2$, 1 $CaCl_2$, 12.5 glucose, and 10 HEPES, titrated to pH 7.4 with NaOH) and patch pipette solutions contained (in mM): 120 K gluconate, 20 KCl, 1.5 MgATP, 5 EGTA, and 10 HEPES (pH 7.3 with KOH). Voltage clamp commands were

controlled using an Axopatch 200B amplifier interfaced to a IBM compatible PC using pClamp 9 software. The liquid-liquid junction potential between the internal and external solution, calculated to be −15 mV, has been corrected for in all experiments. Cell capacitance neutralization and series resistance compensation of ∼80% were used. Current density was measured using a two-step voltage protocol: cells were depolarized from a resting potential of −80 mV to +40 mV for 1 second, then hyperpolarized to −110 mV for 500 ms. Peak tail currents were recorded at −110 mV and normalized relative to cell capacitance. Steady state activation and inactivation and rates of activation/deactivation and inactivation/recovery from inactivation were analyzed as previously described.[20]

Modeling

A Markov state model based on that developed by Kiehn *et al*.[21] was used to reconstruct hERG ionic currents as described in Lu *et al*.[22] The values of the rate constants used in WT-hERG model were as shown in Lu *et. al*.[22] The G572S mutation was modeled by reducing the channel density by 90% to reconstruct the loss of trafficking function. The parameters modified for the hERG model to reproduce the behavior of the G584S channel are summarized in the data supplement.

The Ten Tusscher and Panfilov human ventricular cell action potential (AP) models (epicardial, endocardial, and midmyocardial or M-cell)[23] were modified by removing the original I_{Kr} current component and replacing with the hERG Markov model described above. Numerical time integration was computed as previously described.[22] The size of the current stimuli needed to elicit APs was determined in each case and a stimulus 1.5 times the threshold stimulus was used in all data shown here. Cells were paced at a 1 Hz stimulus rate for 60 seconds to allow the model to reach a steady state, and data shown here are from the time interval 60-61 seconds.

Results

Clinical Features

G572S family: The proband is a 9-year-old French Polynesian female (Fig. 1A) with a history of multiple syncopal episodes. She is adopted and family screening has not been possible to date. Her electrocardiogram (ECG) showed a prolonged QT interval (QTc 570 ms, Fig. 1B) and she had multiple documented cardiac arrests with documented torsade de pointes (Fig. 1C). The proband's brother, a strong swimmer, died suddenly while swimming at the age of 10. The autopsy was negative. The parents and two other siblings are reportedly asymptomatic (no ECGs available), but a paternal uncle has a history of syncope. Genetic screening identified a missense mutation of *KCNH2* resulting in G572S substitution.[17] The coding sequences for *KCNQ1, SCN5A, KCNE1,* and *KCNE2* were all normal.[17] A defibrillator was implanted and high dose beta-blockade initiated.

G584S family: Consists of 19 gene-positive carriers with QTc 452 ± 6 ms (mean ± SEM for n = 14 from whom ECG is available), age 43 ± 16 years, compared to a QTc of 423 ± 8 ms in genotype negative family members (n = 16), age 34 ± 17 years (Fig. 1C). Six of the 19 carriers have had 1 or more syncopal spells, 1 female was resuscitated at the age of 73 and thereafter demonstrated torsade de pointes tachycardia repeatedly; 1 male died during sleep at the age of 56 years. Postmortem studies showed no abnormalities.

Mutant Phenotype

Both G572 and G584 are highly conserved (Fig. 2). Both mutations result in the same amino acid substitution and are located in the pore domain (Fig. 2). Previous analysis of G572S revealed defective trafficking of the hERG channel to the cell surface,[16] but beyond this it was not further characterized. The G584S mutant has not been characterized at a cellular or biophysical level.

Western blot analysis of HEK293 cells transfected with WT-hERG channels showed the expected 2 bands at 135-kDa (immature core-glycosylated form) and 155-kDa (mature complex-glycosylated form)[16,24] (Fig. 3A). G584S channels also showed 2 bands. In contrast, the G572S mutant displayed only a single 135-kDa band (Fig. 3A). Patch clamp analysis of G584S channels showed the typical hook-like currents in response to a 2-step voltage protocol, whereas G572S channels exhibited no currents (Fig. 3B).

Immunofluorescence studies of WT-hERG showed a strong signal in the perinuclear region (consistent with ER localization), additional diffuse staining throughout the cells and the periphery (indicating channel protein progressing from the ER through the Golgi to the plasma membrane), and patches of plasma membrane staining (arrows in [A], Fig. 3C). In contrast, cells expressing G572S only showed strong fluorescence in the perinuclear region, reflecting ER localization (B).

Coassembly of HERG WT and G572S Mutant Subunits

Coimmunoprecipitation experiments indicated association of WT-Flag and G572S-HA hERG (Fig. 4A). Furthermore, this association was observed only for the 135-kDa form, indicating that coassembly of WT and mutant subunits occur in the ER prior to the formation of complex glycosylation. Immunofluorescence experiments also indicated colocalization of G572S and WT-hERG, consistent with retention within the ER (Fig. 4B). Coexpression of G572S and WT-hERG also resulted in a marked diminution of the 155-kDa band for the WT channel (Fig. 4C).

To assess the effects of coexpression of G572S with WT-hERG on hERG current density we utilized a CHO cell line stably expressing WT-hERG channels[25] that was transiently transfected with WT-hERG, G572S-hERG or blank vector. The current density in the blank vector transfected cells was 42 ± 5 pA/pF (n = 8). Transient transfection of WT-hERG into this cell line resulted in the expected doubling of hERG current density to 81 ± 26 pA/pF (n = 6). Conversely, transient transfection of G572S-hERG channels resulted in a decrease in current density to 8 ± 2 pA/pF (n = 7), that is, ∼90% reduction in current density compared to the WT + WT cells (Fig. 4D).

The data for the current density for WT ± G572S-hERG and the data for the proportion of fully glycosylated protein versus core-glycosylated protein versus the ratio of G572S:WT subunits are plotted in Figure 4E. The lines in Figure 4E indicate the proportion of tetramers containing at least 1 mutant subunit for random coassembly (solid) and no-coassembly (dashed) of mutant and WT subunits. These data in Figure 4E are consistent with a single G572S

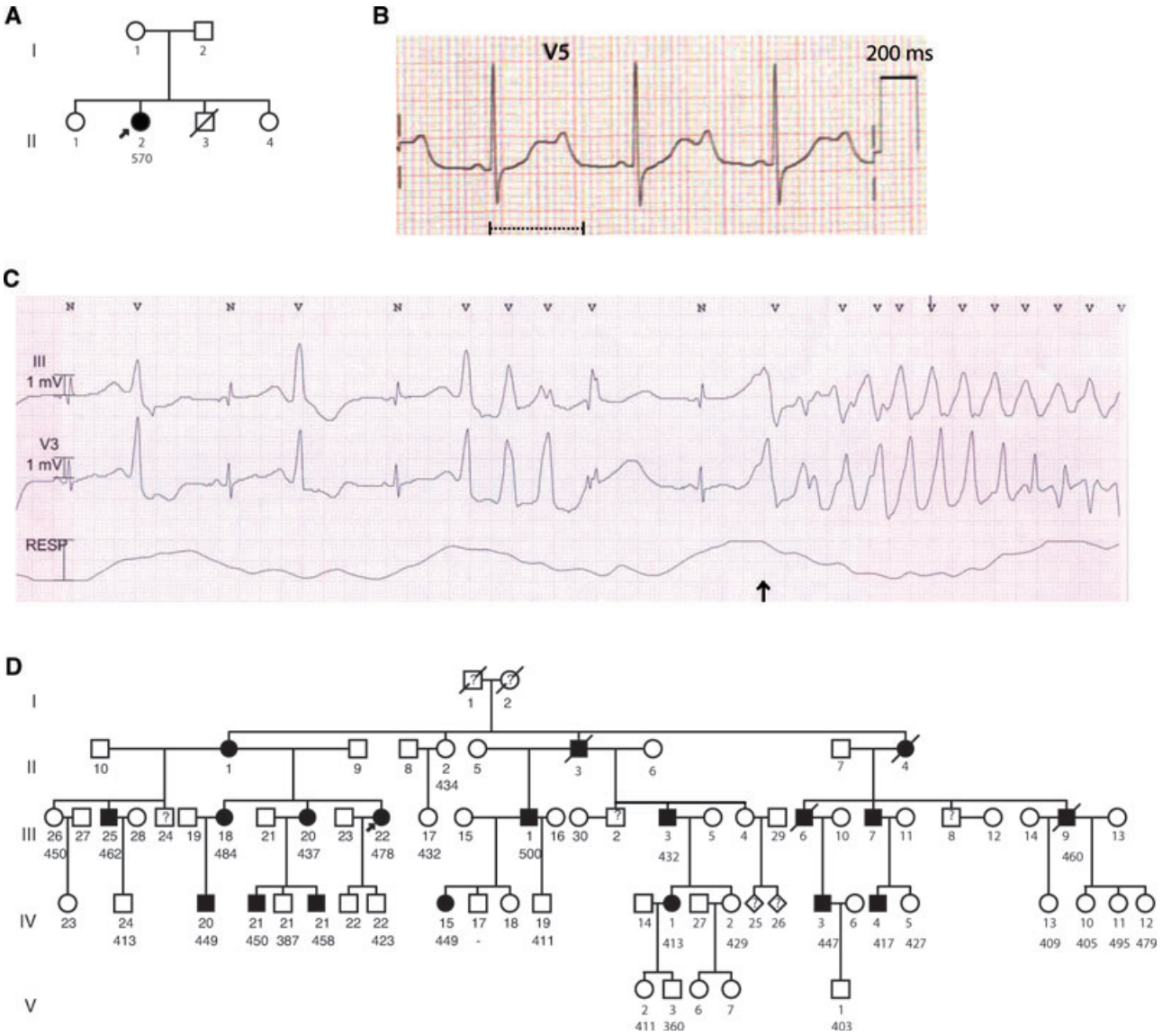

Figure 1. *Clinical features of affected families. (A) Pedigree for G572S family. The proband (II:2), indicated by arrow, had a QTc of 570 ms (see B). Electrocardiograms (ECGs) were not available for other family members. The proband's brother died suddenly, aged 10. (B) Recording from lead V5 of a 12-lead ECG from the G572S family proband. The horizontal bar at top right indicates 200 ms. The dotted line indicates the QT interval, which in this case was 500 ms corresponding to a QTc of 570 ms (for RR interval of 770 ms). (C) Rhythm strip obtained during an episode of torsade de pointes in same patient as depicted in (B). N indicates normal beat, V indicates ectopic beat, and vertical arrow indicates commencement of torsade de pointes. (D) Pedigree for G584S family. Proband (III:22) is indicated by arrow. Where available, QTc values are shown below each individual. Filled symbols indicate genotype-positive individuals.*

subunit resulting in a null channel, that is, dominant negative suppression.

Electrophysiological Phenotype of G584S

The largest change in the properties of G584S-hERG compared to WT-hERG was an ~ -20 mV shift in the voltage dependence of steady-state inactivation (Fig. 5 and Table 1). Conversely, there was no alteration to the voltage dependence of activation (Table 1) and only modest, but significant, changes to the kinetics of activation and inactivation (Table 1).

To investigate the functional significance of the perturbations to hERG kinetics caused by the G584S mutation we recorded currents in response to AP voltage waveforms, as previously described.[22] Typical examples of current traces recorded from G584S- and WT-hERG channels in response to a ventricular AP waveform are shown (gray and black lines, respectively) in Figure 5C. The lower current seen in the G584S transfected cells reflects the fact that in the voltage range of ventricular repolarization (-10 to -85 mV) G584S-hERG channels are still predominantly inactivated ($V_{0.5}$ inact $= -99$ mV, Table 1), whereas WT-hERG channels have largely recovered from inactivation by -85 mV ($V_{0.5}$ inact $= -79$ mV, Table 1).

Coexpression of WT- with G584S-hERG resulted in an intermediate phenotype; for example, the half voltage for steady state inactivation was -88.4 ± 1.2 mV (n = 4) compared to -79.8 ± 0.7 mV for WT and -99.3 ± 1 mV for G584S-hERG alone (Table 1).

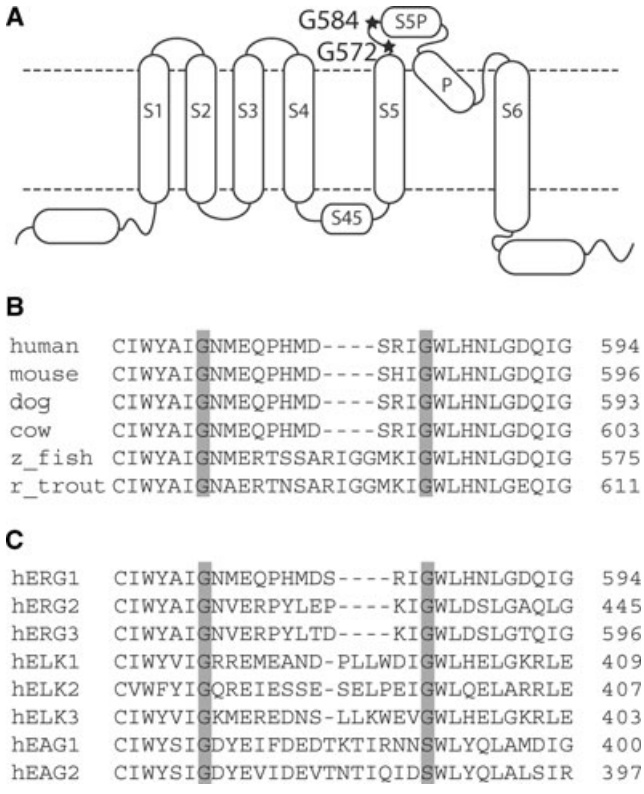

Figure 2. *Location of G572S and G584S mutants. (A) Topology of hERG subunit highlighting 6 transmembrane domains (labeled S1 to S6), pore helix (P), helix between S4 and S5 (S45), and helix between S5 and P (S5P). Locations of residues G572 and G584 in the segment between the S5 and S5P helices are shown by stars. (B) Alignment of hERG sequences illustrating 100% conservation of G572 and G584 in the species shown. (C) Alignment of human sequences for the ether-a-go-go (EAG) subfamily of K^+ channels illustrating 100% conservation of G572. G584 is conserved among the ether-a-go-go-related (ERG) and ether-a-go-go-like (ELK), but not EAG subfamily.*

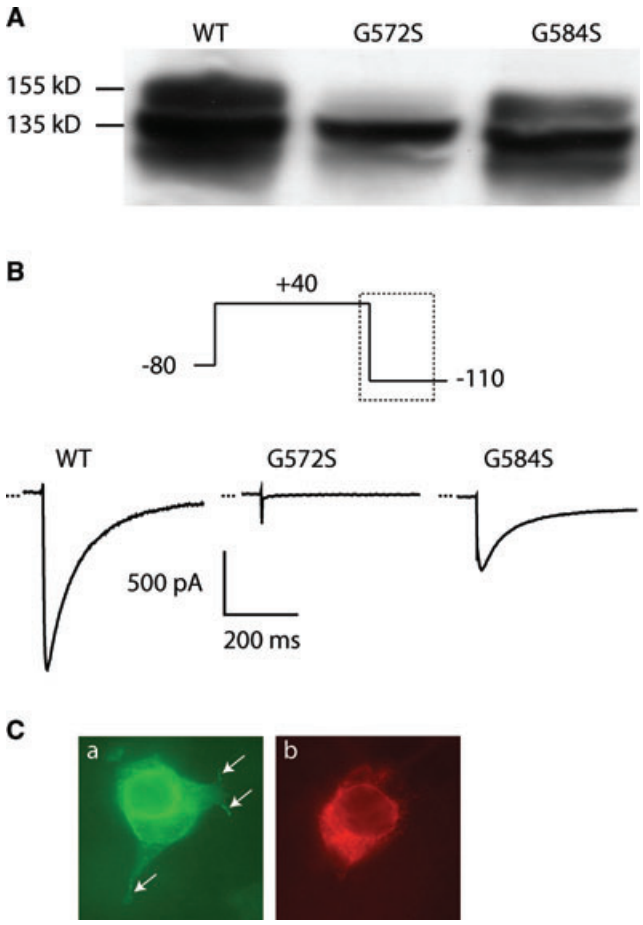

Figure 3. *Classification of G572S and G584S mutants. (A) Typical example of western blots for WT-, G572S- and G584S-hERG channels. Bands at 155 kD and 135 kD are highlighted. (B) Typical current traces recorded from cells transfected with WT, G572S, or G584S-hERG channels. (C) Typical immunofluorescence images from cells transfected with (a) WT-, (b) G572S-hERG. Arrows indicate plasma membrane location for WT channels.*

Modeling of Mutant Phenotypes

Figure 6 illustrates simulated APs from the Ten Tusscher human ventricular model[23] for epicardial (red), endocardial (blue), and M cells (black) for WT, G572S (WT-hERG channel density reduced to 10%) and the heterozygous G584S mutation. As expected, there is a more pronounced lengthening of the AP duration for the G572S than for the G584S mutant and these effects are most readily apparent in the M-cell APs.

It has been proposed that hERG K^+ channels may be important for suppression of premature beats.[22,26] Figure 6B shows the effect of a premature stimulus given at (1) the point of 90% repolarization (APD_{90}, red lines) and (2) the most closely coupled premature stimulus that could elicit an AP (blue lines). For WT cells, the shortest interval that could elicit an AP was APD_{90} + 25 ms, for WT/G584S it was APD_{90} +23 ms, and for WT/G572S, a stimulus at APD_{90} −60 ms could elicit a regenerative AP waveform.

Discussion

Cardiac arrhythmias are a major cause of morbidity and mortality. Implantable defibrillators have become the mainstay of treatment aimed at reducing the incidence of sudden cardiac death. What remains elusive though is the ability to accurately identify those individuals at greatest risk of sudden cardiac death.[14,27] Patients with LQTS provide a well-defined subset of patients at risk of sudden cardiac death, and the condition has been aptly described as the "Rosetta Stone of sympathetic mediated ventricular arrhythmias."[28] To date, risk stratification in LQTS has utilized a range of clinical,[3,4] electrocardiographic,[6] and genetic markers.[8,10,11,29] In this study, we investigated whether biophysical and modeling studies of two hERG mutations could assist with stratifying risk relative to family history.

Phenotype of the G572S Mutation

G572 is a highly conserved residue in the pore domain (Fig. 2). Despite the unavailability of complete clinical data for the patient with this mutation, it is apparent that she has a severe phenotype, that is, early onset of symptoms (∼5 years of age), significantly prolongation of the QT interval and documented evidence of torsade de pointes arrhythmias (Fig.1). In addition, a first-degree relative (presumably with the same mutation) died suddenly at the age of 10 years. This is consistent with pore-mutations in hERG being high risk.[29] Conversely, both parents appeared to be

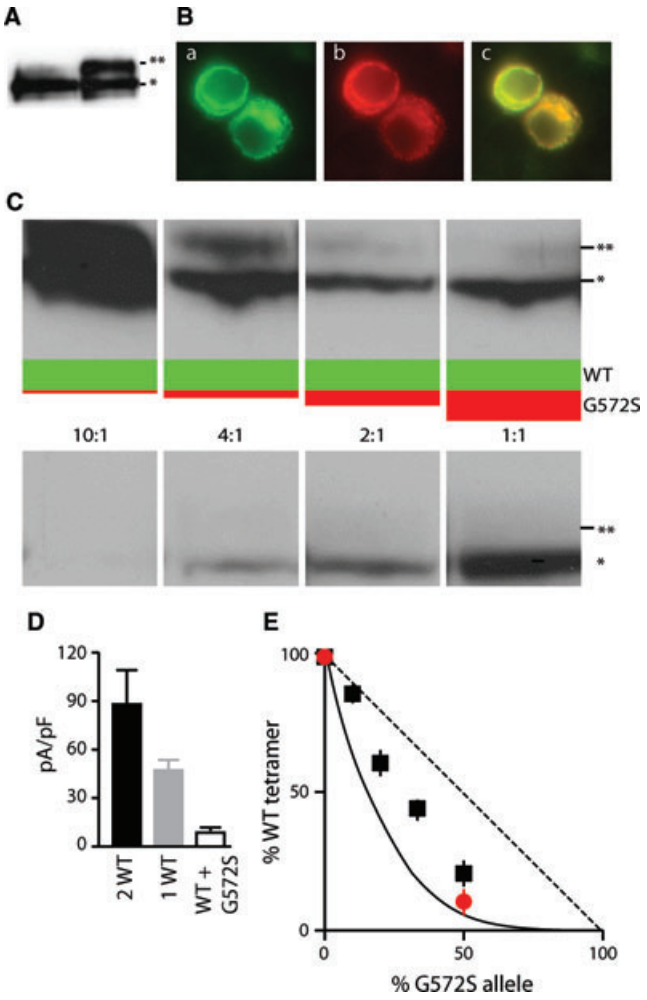

Figure 4. *Coassembly of WT- and G572S-hERG channels. (A) Lane 1 immunoprecipitation of WT-Flag with G572S-HA results in only a single band at 135 kD. Lane 2 control: Immunoprecipitation of WT-Flag with WT-HA gives the expected 2 bands at 155 kD and 135 kD. (B) Typical immunofluorescence images from cells cotransfected with WT and G572S-hERG and probed with (a) anti-HA to detect G572S or (b) anti-Flag to detect WT and (c) overlay showing colocalization. (C) Typical Western blots for cells transfected with different ratios of WT:G572S-hERG (all experiments performed on same day with same cDNA preparation). The top panel blotted with anti-Flag antibody to detect WT subunits and bottom panel blotted with anti-HA antibody to detect G572S subunits. The boxes between the panels indicate relative levels of expression of WT (green) and G572S (red) subunits. **155 kD, *135 kD. (D) Current density for WT+WT: 81 ± 26 pA/pF (n = 6); WT + Blank vector: 42 ± 5 pA/pF (n = 8); WT + G572S-hERG: 8 ± 2 pA/pF (n = 7). (E) Plot of ratio of 155 kD/135 kD band (black symbols) and relative current density (red symbols) for different percentages of WT and G572S subunits. Lines indicate the%tetramers formed exclusively of WT monomers assuming random association (solid) or no association (dashed) with G572S subunits.*

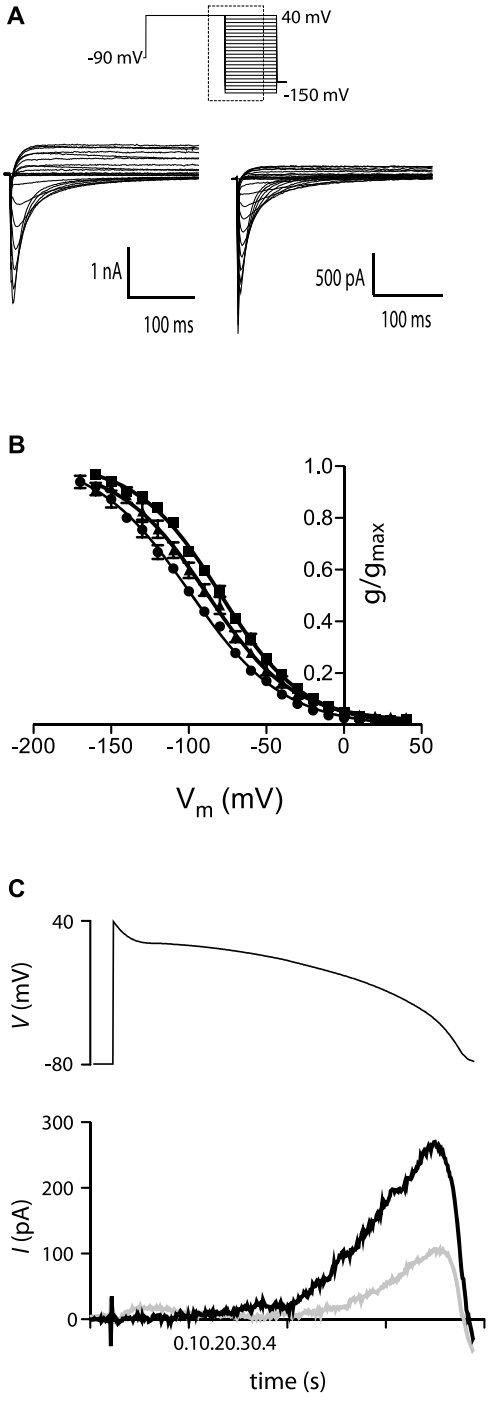

Figure 5. *Electrophysiology of G584S-hERG channels. (A) Typical example of currents recorded from (i) WT- and (ii) G584S-hERG channels during a two-step voltage protocol (shown in inset) to measure steady-state inactivation. (B) Summary data (mean ± SEM) for the voltage dependence of steady-state inactivation for WT-, G584S- and WT + G584S-hERG channels. (C) Typical example of currents recorded from (i) WT and (ii) G584S-hERG channels during ventricular action potential (AP) clamp protocols (AP waveform shown in inset).*

asymptomatic, yet presumably one of them carries the mutation. If one of the parents does have the mutation, then this would suggest that penetrance in this kindred is quite low.[30] However, in the absence of a confirmed genotype or indeed ECG data from either parent it is impossible to draw any firm conclusions based on the clinical data alone.

In vitro studies showed that the G572S-hERG channel had a trafficking defect, as also shown by Anderson *et al.*[16] In addition to this, however, we examined how the presence of G572S hERG subunits affected trafficking of WT subunits in the context of heterozygous expression. These experiments showed that the G572S-hERG channel subunits can coassemble with WT subunits (Fig. 4), and this results in retention of WT subunits within the ER (Fig. 4). Quantification of the association between G572S-hERG and WT-hERG subunits

TABLE 1

Kinetic Parameters for G584S-hERG

	WT (n = 4–6)	G584S (n = 4–6)
$V_{0.5,\,act}$ (mV)	−15.5 ± 1.7	−15.4 ± 1.5
$V_{0.5,\,inact}$ (mV)	−79.8 ± 0.7	−99.3 ± 1.0*
$\tau_{act,\,0\,mV}$ (ms)	503 ± 66	355 ± 38*
$\tau_{deact,\,-80\,mV}$ (ms)	260 ± 52	163 ± 37*
$\tau_{inact,\,0\,mV}$ (ms)	11.9 ± 0.8	7.7 ± 1.0*
$\tau_{recover,\,-80\,mV}$ (ms)	11.7 ± 1.5	7.8 ± 0.7*

*P < 0.05 compared to WT.

indicates that the presence of a single G572S subunit in a heterotetramer complex is sufficient to cause loss of function (Fig. 4E). A patient with a heterozygote G572S-hERG mutation would therefore have <10% of the hERG current density compared to a normal control. *In silico* modeling indicated that this mutation would cause a significant prolongation of the AP duration (Fig. 6A) and make the patient vulnerable to premature stimuli delivered at closely coupled intervals (Fig. 6B), that is, so-called R-on-T premature beats.[31] Overall, the *in vitro* data indicate that the G572S mutation is an intrinsically severe mutation.

Phenotype of the G584S Mutation

G584 is a highly conserved residue in the pore domain, suggesting that the mutation might be malignant.[29] However, clinically, the patients had a mild phenotype with only modest QT interval prolongation (QTc 460 ms) and only 6 of 19 carriers exhibiting syncopal episodes. Of the 2 reported deaths, both were relatively elderly (56 years and 78 years). The variability in clinical presentation in this kindred is again consistent with the previously reported variable penetrance in the LQTS.[30]

Disease causing ion channel mutations can be classified into 4 types, I: abnormal mRNA synthesis, II: protein trafficking defect, III: abnormal ion permeation, and IV: abnormal gating.[32] Over 90% of the LQTS-associated missense mutations in hERG, characterized to date, result in abnormal trafficking (see e.g.,[16]). The Western blot data shown in Figure 3 suggested that there could be an impairment of trafficking in the G584S mutant. However, patch clamp assays of channel trafficking, estimated from current density measurements, did not show any difference between WT and G584S-hERG channels. This suggests that there is no significant trafficking defect in the G584S channels. Conversely, the G584S mutant channels clearly have a significant gating defect (Fig. 5). A number of LQTS associated hERG mutants have been shown to have abnormal inactivation when expressed in Xenopus oocytes (e.g., T474I, A614V, V630L)[33] but subsequently shown to have a trafficking defect when expressed in mammalian cell lines.[16] There are a number of missense mutations that have a gating phenotype when expressed in mammalian cells, for example, R56Q[34] and M124R[35] have accelerated deactivation and L552S has a complex gating phenotype.[36] The data reported here for the G584S hERG mutant channel is the first example of a long-QT-associated missense mutant that has a genuine type IV phenotype, that is, abnormal gating,[32] due to enhanced inactivation (Fig. 5).

Coexpression of WT and G584S-hERG channels caused an intermediate phenotype that resulted in ∼30% reduction in current during repolarization of the cardiac AP. Such a reduction would be associated with only a modest prolongation of the ventricular AP (as confirmed by modeling studies). Furthermore, the response to premature stimuli was very similar for WT and G584S heterozygote cells. In summary, the *in vitro* data and modeling suggest the G584S mutation has an intrinsically mild phenotype.

Conclusions

The results from this study show that 2 LQTS2 mutations that are seemingly very similar, that is, very similar location and same change in amino acid, can have very different phenotypes. In general, mutations in the pore domain are associated with a more severe outcome,[29] and this appears to be the case for the G572S mutation. However, the G584S mutation appears to be an exception to this rule. Furthermore, the G584S mutation represents the first hERG mutation where the cause of disease can be attributed to enhanced inactivation, unlike the cases of T474I, A614V, and V630L, which have abnormal inactivation[33] but where the primary mechanism of disease is abnormal trafficking.[16] Stratification of

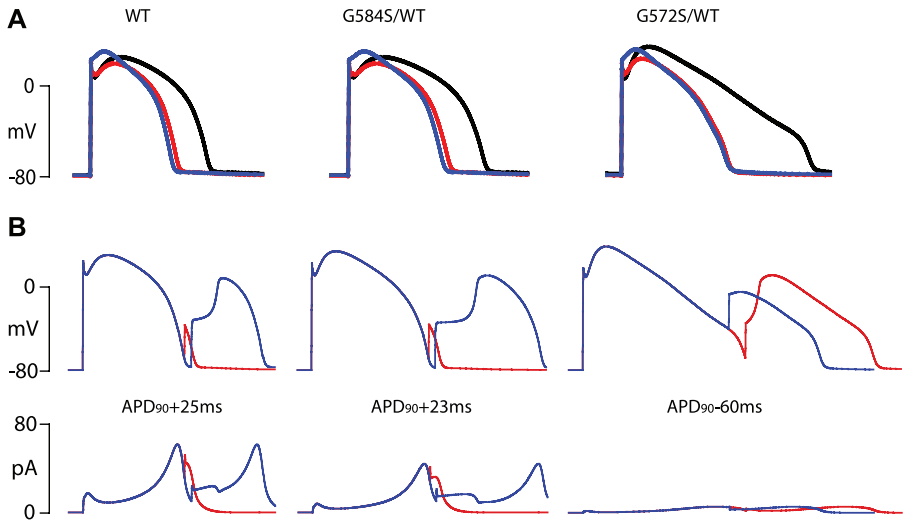

Figure 6. *Modeled ventricular action potentials (APs) for WT and mutant hERG channels. (A) Modeled AP waveforms (epicardial, red; endocardial, blue; M-cells, black) generated using the Ten Tusscher human ventricular AP model[22] with hERG current generated by either the WT-hERG Markov model[22] or the G584S Markov model (see data supplement). WT-hERG current density was reduced to 10% to simulate the heterozygote G572S-hERG scenario. (B) Modeled response to premature stimuli for WT-, G572S- and G584S-hERG modeled M-cell APs (upper panel) and hERG current (lower panel). Premature stimuli were delivered at APD_{90} (red) or at the shortest coupling interval that would elicit an action potential (blue).*

risk in patients with LQTS is often difficult as in many instances affected kindreds are small, present with variable clinical features,[30] and/or there are incomplete clinical data available. Our study indicates that determining the intrinsic severity of a given mutation using *in vitro* assays in combination with *in silico* modeling will be another useful tool for stratifying risk, although this hypothesis should be further investigated in a larger cohort of kindreds.

Acknowledgments: We thank Tadeusz Marciniec for expert technical assistance. We also thank Stefan Mann and Raj Subbiah for helpful discussions.

References

1. Roden DM: Clinical practice. Long-QT syndrome. N Engl J Med 2008;358:169-176.
2. Moss AJ, Schwartz PJ: 25th anniversary of the International Long-QT Syndrome Registry: An ongoing quest to uncover the secrets of long-QT syndrome. Circulation 2005;111:1199-1201.
3. Goldenberg I, Moss AJ, Peterson DR, McNitt S, Zareba W, Andrews ML, Robinson JL, Locati EH, Ackerman MJ, Benhorin J, Kaufman ES, Napolitano C, Priori SG, Qi M, Schwartz PJ, Towbin JA, Vincent GM, Zhang L: Risk factors for aborted cardiac arrest and sudden cardiac death in children with the congenital long-QT syndrome. Circulation 2008;117:2184-2191.
4. Locati EH, Zareba W, Moss AJ, Schwartz PJ, Vincent GM, Lehmann MH, Towbin JA, Priori SG, Napolitano C, Robinson JL, Andrews M, Timothy K, Hall WJ: Age- and sex-related differences in clinical manifestations in patients with congenital long-QT syndrome: Findings from the International LQTS Registry. Circulation 1998;97:2237-2244.
5. Sauer AJ, Moss AJ, McNitt S, Peterson DR, Zareba W, Robinson JL, Qi M, Goldenberg I, Hobbs JB, Ackerman MJ, Benhorin J, Hall WJ, Kaufman ES, Locati EH, Napolitano C, Priori SG, Schwartz PJ, Towbin JA, Vincent GM, Zhang L: Long QT syndrome in adults. J Am Coll Cardiol 2007;49:329-337.
6. Priori SG, Schwartz PJ, Napolitano C, Bloise R, Ronchetti E, Grillo M, Vicentini A, Spazzolini C, Nastoli J, Bottelli G, Folli R, Cappelletti D: Risk stratification in the long-QT syndrome. N Engl J Med 2003;348:1866-1874.
7. Splawski I, Shen J, Timothy KW, Lehmann MH, Priori S, Robinson JL, Moss AJ, Schwartz PJ, Towbin JA, Vincent GM, Keating MT: Spectrum of mutations in long-QT syndrome genes. KVLQT1, HERG, SCN5A, KCNE1, and KCNE2. Circulation 2000;102:1178-1185.
8. Zareba W, Moss AJ, Schwartz PJ, Vincent GM, Robinson JL, Priori SG, Benhorin J, Locati EH, Towbin JA, Keating MT, Lehmann MH, Hall WJ: Influence of genotype on the clinical course of the long-QT syndrome. International Long-QT Syndrome Registry Research Group. N Engl J Med 1998;339:960-965.
9. Crotti L, Spazzolini C, Schwartz PJ, Shimizu W, Denjoy I, Schulze-Bahr E, Zaklyazminskaya EV, Swan H, Ackerman MJ, Moss AJ, Wilde AA, Horie M, Brink PA, Insolia R, De Ferrari GM, Crimi G: The common long-QT syndrome mutation KCNQ1/A341V causes unusually severe clinical manifestations in patients with different ethnic backgrounds: Toward a mutation-specific risk stratification. Circulation 2007;116:2366-2375.
10. Shimizu W, Horie M, Ohno S, Takenaka K, Yamaguchi M, Shimizu M, Washizuka T, Aizawa Y, Nakamura K, Ohe T, Aiba T, Miyamoto Y, Yoshimasa Y, Towbin JA, Priori SG, Kamakura S: Mutation site-specific differences in arrhythmic risk and sensitivity to sympathetic stimulation in the LQT1 form of congenital long QT syndrome: Multicenter study in Japan. J Am Coll Cardiol 2004;44:117-125.
11. Moss AJ, Shimizu W, Wilde AA, Towbin JA, Zareba W, Robinson JL, Qi M, Vincent GM, Ackerman MJ, Kaufman ES, Hofman N, Seth R, Kamakura S, Miyamoto Y, Goldenberg I, Andrews ML, McNitt S: Clinical aspects of type-1 long-QT syndrome by location, coding type, and biophysical function of mutations involving the KCNQ1 gene. Circulation 2007;115:2481-2489.
12. Sanguinetti MC, Curran ME, Spector PS, Keating MT: Spectrum of HERG K+-channel dysfunction in an inherited cardiac arrhythmia. Proc Natl Acad Sci USA 1996;93:2208-2212.
13. Goldenberg I, Moss AJ: Long QT syndrome. J Am Coll Cardiol 2008;51:2291-2300.
14. Moss AJ, Goldenberg I: Importance of knowing the genotype and the specific mutation when managing patients with long-QT syndrome. Circ Arrhythmia Electrophysiol 2008;117:219-226.
15. Soreq H, Seidman S: Xenopus oocyte microinjection: From gene to protein. Methods Enzymol 1992;207:225-265.
16. Anderson CL, Delisle BP, Anson BD, Kilby JA, Will ML, Tester DJ, Gong Q, Zhou Z, Ackerman MJ, January CT: Most LQT2 mutations reduce Kv11.1 (hERG) current by a class 2 (trafficking-deficient) mechanism. Circulation 2006;113:365-373.
17. Chung SK, MacCormick JM, McCulley CH, Crawford J, Eddy CA, Mitchell EA, Shelling AN, French JK, Skinner JR, Rees MI: Long QT and Brugada syndrome gene mutations in New Zealand. Heart Rhythm 2007;4:1306-1314.
18. Laitinen P, Fodstad H, Piippo K, Swan H, Toivonen L, Viitasalo M, Kaprio J, Kontula K: Survey of the coding region of the HERG gene in long QT syndrome reveals six novel mutations and an amino acid polymorphism with possible phenotypic effects. Hum Mutat 2000;15:580-581.
19. Clarke CE, Hill AP, Zhao J, Kondo M, Subbiah RN, Campbell TJ, Vandenberg JI: Effect of S5P alpha-helix charge mutants on inactivation of hERG K+ channels. J Physiol 2006;573:291-304.
20. Vandenberg JI, Varghese A, Lu Y, Bursill JA, Mahaut-Smith MP, Huang CL: Temperature dependence of human ether-a-go-go-related gene K+ currents. Am J Physiol Cell Physiol 2006;291:C165-C175.
21. Kiehn J, Lacerda AE, Brown AM: Pathways of HERG inactivation. Am J Physiol 1999;277:H199-H210.
22. Lu Y, Mahaut-Smith MP, Varghese A, Huang CL, Kemp PR, Vandenberg JI: Effects of premature stimulation on HERG K(+) channels. J Physiol 2001;537:843-851.
23. Ten Tusscher KH, Panfilov AV: Cell model for efficient simulation of wave propagation in human ventricular tissue under normal and pathological conditions. Phys Med Biol 2006;51:6141-6156.
24. Zhou Z, Gong Q, Epstein ML, January CT: HERG channel dysfunction in human long QT syndrome. Intracellular transport and functional defects. J Biol Chem 1998;273:21061-21066.
25. Walker BD, Valenzuela SM, Singleton CB, Tie H, Bursill JA, Wyse KR, Qiu MR, Breit SN, Campbell TJ: Inhibition of HERG channels stably expressed in a mammalian cell line by the antianginal agent perhexiline maleate. Br J Pharmacol 1999;127:243-251.
26. Smith PL, Baukrowitz T, Yellen G: The inward rectification mechanism of the HERG cardiac potassium channel. Nature 1996;379:833-836.
27. Vincent GM: Genotyping has a minor role in selecting therapy for congenital long-QT syndromes at present. Circ Arrhythmia Electrophysiol 2008;117:227-233.
28. Zipes DP: The long QT interval syndrome. A Rosetta stone for sympathetic related ventricular tachyarrhythmias. Circulation 1991;84:1414-1419.
29. Moss AJ, Zareba W, Kaufman ES, Gartman E, Peterson DR, Benhorin J, Towbin JA, Keating MT, Priori SG, Schwartz PJ, Vincent GM, Robinson JL, Andrews ML, Feng C, Hall WJ, Medina A, Zhang L, Wang Z: Increased risk of arrhythmic events in long-QT syndrome with mutations in the pore region of the human ether-a-go-go-related gene potassium channel. Circulation 2002;105:794-799.
30. Priori SG, Napolitano C, Schwartz PJ: Low penetrance in the long-QT syndrome: Clinical impact. Circulation 1999;99:529-533.
31. Benhorin J, Medina A: Images in clinical medicine. Congenital long-QT syndrome. N Engl J Med 1997;336:1568.
32. Delisle BP, Anson BD, Rajamani S, January CT: Biology of cardiac arrhythmias: Ion channel protein trafficking. Circ Res 2004;94:1418-1428.
33. Nakajima T, Furukawa T, Tanaka T, Katayama Y, Nagai R, Nakamura Y, Hiraoka M: Novel mechanism of HERG current suppression in LQT2: Shift in voltage dependence of HERG inactivation. Circ Res 1998;83:415-422.
34. Berecki G, Zegers JG, Verkerk AO, Bhuiyan ZA, de Jonge B, Veldkamp MW, Wilders R, van Ginneken AC: HERG channel (dys)function revealed by dynamic action potential clamp technique. Biophys J 2005;88:566-578.
35. Shushi L, Kerem B, Goldmit M, Peretz A, Attali B, Medina A, Towbin JA, Kurokawa J, Kass RS, Benhorin J: Clinical, genetic, and electrophysiologic characteristics of a new PAS-domain HERG mutation (M124R) causing long QT syndrome. Ann Noninvasive Electrocardiol 2005;10:334-341.
36. Piippo K, Laitinen P, Swan H, Toivonen L, Viitasalo M, Pasternack M, Paavonen K, Chapman H, Wann KT, Hirvela E, Sajantila A, Kontula K: Homozygosity for a HERG potassium channel mutation causes a severe form of long QT syndrome: Identification of an apparent founder mutation in the Finns. J Am Coll Cardiol 2000;35:1919-1925.